

# Quantum circuit algorithm for topological invariants of second-order topological many-body quantum magnets

Sebastián Domínguez-Calderón,<sup>1,2</sup> Marcel Niedermeier,<sup>1</sup> Jose L. Lado,<sup>1</sup> and Pascal M. Vecsei<sup>1,3</sup>

<sup>1</sup>*Department of Applied Physics, Aalto University, 00076 Aalto, Finland*

<sup>2</sup>*School of Natural Sciences, Technische Universität München, D-85748 Garching, Germany*

<sup>3</sup>*Institute of Mechanical Engineering and Energy Technology,*

*Lucerne University of Applied Science and Arts, CH-6002 Lucerne, Switzerland*

(Dated: December 23, 2025)

Topological quantum matter represents a flexible playground to engineer unconventional excitations. While non-interacting topological single-particle systems have been studied in detail, topology in quantum many-body systems remains an open problem. Specifically, in the quantum many-body limit, one of the challenges lies in the computational complexity of obtaining the many-body ground state and its many-body topological invariant. While algorithms to compute ground states with quantum computers have been heavily investigated, algorithms to compute topological invariants in a quantum computer are still under active development. Here we demonstrate a quantum circuit to compute the many-body topological invariant of a second-order topological quantum magnet encoded in qubits. Our algorithm relies on a quantum circuit adiabatic evolution in transverse paths in parameter space, and we uncover hidden topological invariants depending on the traversed path. Our work puts forward an algorithm to leverage quantum computers to characterize many-body topological quantum matter.

## I. INTRODUCTION

With the advent of topological materials and their vast array of new physical phenomena [1, 2], intense research has been devoted to their understanding and classification. Among them, symmetry protected topological (SPT) phases hold promise for engineering fault-tolerant quantum computing and spintronic devices [1, 3, 4]. SPT phases are hard to distinguish from trivial phases due to their subtle nature [2], which means that they are generally not detectable by local order parameters and have no obvious distinction merely based on symmetry arguments [3]. SPTs are found in free-particle systems as well as in strongly-interacting matter such as topological crystalline quantum magnets [5]. 1D and 2D gapped SPT phases have a full classification using group cohomology theory, and higher-dimensional generalizations have been developed [6, 7]. While SPT phases in non-interacting systems are well understood [6–8], many-body interacting systems remain a substantial open challenge [3, 9].

The discovery of higher-order topological phases in non-interacting fermions enabled new exotic phenomena such as corner and hinge states [10–13], which generalize the bulk-boundary correspondence of conventional topological insulators. Higher-order topological phases now have exhaustive classification for non-interacting systems [14]. Theoretical models in interacting systems have also been shown to exhibit phenomena similar to higher-order topological phases [15]. Higher-order symmetry-protected topological (HOSPT) phases can be built from lower-dimensional SPTs in a systematic way, and to a large extent can be classified using group cohomology [16], which provides frameworks for calculating topological invariants using algebraic topology and cocycles of group cohomology [17, 18]. HOSPT states appearing in interacting bosonic and fermionic systems can exhibit

corner modes [19], and have attracted substantial attention over the last few years [20–30].

Despite the existence of theoretical and computational methods to calculate topological invariants in non-interacting systems, the many-body case is an exponentially hard problem [31]. Quantum computers are a natural candidate in the calculation of topological invariants of many-body Hamiltonians, for which a variety of algorithms to compute ground states have been developed [32–34]. When dealing with a topological system, not only the ground state, but also its topological invariant becomes a crucial object to be computed [17, 35]. This has motivated a variety of quantum circuit algorithms for topological phases of matter in both non-interacting and interacting systems [36–42]. As such, quantum computers hold potential for classifying, computing and predicting many-body topological quantum matter, and, specifically, interacting HOSPT phases.

In this work, we present a quantum circuit to compute topological invariants in higher-order symmetry protected topological phases. Specifically, we demonstrate our algorithm for computing the quantized Berry phase of a first-order, as well as a second-order SPT quantum magnet, both of which are described by a Heisenberg spin-1/2 model. The 2D tetramerized case exhibits a plaquette structure of bonds (Fig. 3), while the 1D dimerized case exhibits an alternating link structure (Fig. 2). For such systems with anti-unitary symmetry (in this case time-reversal), the Berry phase topological invariant is quantized to 0 or  $\pi$ , corresponding to a trivial phase and a HOSPT phase, respectively. Topological invariants are calculated by simulating time-evolution via gate-based adiabatic quantum circuits, and extracting the Berry phase by means of a Hadamard test. Our results show the use case of quantum computing to classify higher-order symmetry protected topological phases phases, highlight-

ing their potential for finding new phases of matter.

## II. METHODS

To detect the topological phase transitions, we exploit specific geometric phases emerging during a cyclic evolution in a given parameter space. This geometric phase, known as the Berry phase in non-interacting problems, can be generally defined as follows. The Berry phase emerges as a general solution of adiabatic state evolution of a parametrized Hamiltonian  $H(\mathbf{q})$ , dependent on a set of parameters  $\mathbf{q} = (q_1, q_2, \dots, q_n)$  [43, 44], which without loss of generality are defined within a circle,  $q_i \in [0, 2\pi]$ . For each set of parameters, there exists a complete set of eigenstates such that

$$H(\mathbf{q}) |n(\mathbf{q})\rangle = E_n(\mathbf{q}) |n(\mathbf{q})\rangle. \quad (1)$$

According to the adiabatic theorem, if the system is initialized in an eigenstate  $|n(\mathbf{q})\rangle$ , then a slow evolution of the Hamiltonian parameters will keep the state vector in the instantaneous eigenstate  $|n(\mathbf{q}(t))\rangle$  at all times. Considering an adiabatic time evolution, where parameters follow a closed path, eigenstates will pick up a total phase consisting of the difference between the dynamical phase  $\varphi_D$  and the geometrical (Berry) phase  $\varphi_B$

$$U(0, T) |n(\mathbf{q})\rangle = e^{-i(\varphi_D - \varphi_B)} |n(\mathbf{q})\rangle, \quad (2)$$

where  $U(0, T)$  denotes a time evolution from time 0 to  $T$ ,

$$U(0, T) = \mathcal{T} \left\{ e^{-\frac{i}{\hbar} \int_0^T dt H(\mathbf{q}(t))} \right\}, \quad (3)$$

where  $\mathcal{T}$  is the time ordering operator and the phases  $\varphi_D$ ,  $\varphi_B$  are given by

$$\varphi_D = \int_0^T dt E_n(\mathbf{q}(t)), \quad (4)$$

$$\varphi_B = i \int_0^T dt \langle n(\mathbf{q}(t)) | \partial_t |n(\mathbf{q}(t))\rangle. \quad (5)$$

Considering a general anti-unitary operator  $\Phi = KU$ , where  $K$  denotes complex conjugation and  $U$  is some unitary operator, it holds that its action on the Berry phase is  $\Phi : \varphi_B \rightarrow -\varphi_B$ . If the Hamiltonian in consideration has anti-unitary symmetry  $[H, \Phi] = 0$ , then the Berry phase must respect the symmetry  $\varphi_B = -\varphi_B$ . However, it is known that the Berry phase must be gauge invariant within a circle (modulo  $2\pi$ ). Both gauge invariance and anti-unitary symmetry quantize the Berry phase to  $\varphi_B = \{0, \pi\}$  [45].

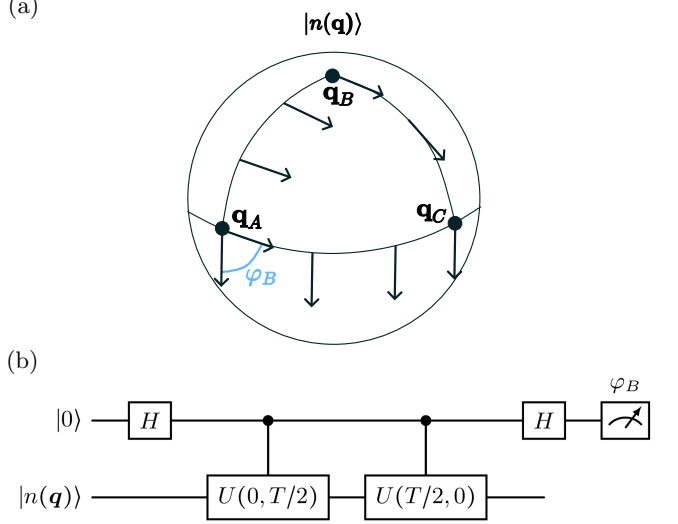


FIG. 1. (a) An instantaneous eigenstate evolved along a closed parameter path will pick up a Berry phase, which is a measure of how the complex vector changes along the path. This effect is analogous to parallel transport of vectors in curved geometry. (b) Proposed quantum circuit with a Hadamard test on an adiabatic time evolution  $U(t_0, t_1)$  which allows to measure  $\varphi_B$ .

To isolate the Berry phase, we can evolve the system back in time to cancel the dynamical phase, since it is anti-symmetric in time  $\int_T^0 dt E(\mathbf{q}(t)) = -\varphi_D$  [37]. The total phase picked up by an instantaneous eigenstate, after evolving forwards and then backwards in time, is twice the Berry phase

$$U(T, 0)U(0, T) |n(\mathbf{q})\rangle = e^{i2\varphi_B} |n(\mathbf{q})\rangle, \quad (6)$$

which is understood as a consequence of double looping the parameter space and the dynamical phase being canceled. For time-reversal symmetric Hamiltonians (also an anti-unitary symmetry), time evolution can be cut into half periods, such that time goes forward and backwards while the parameters perform only a single loop, allowing to distinguish the quantization  $\varphi_B = \{0, \pi\}$  [37] as

$$U(0, T/2)U(T/2, 0) |n(\mathbf{q})\rangle = e^{i\varphi_B} |n(\mathbf{q})\rangle. \quad (7)$$

We implement adiabatic time evolution in a quantum circuit by dividing the Hamiltonian into parts  $H(t) = H_1(t) + \dots + H_q(t)$ , where each part  $H_q$  consists of only commuting operators. We then cut up time evolution into a sequence of small steps following the second-order Trotter-Suzuki decomposition [46, 47]

$$U_2(t + \Delta t) \approx e^{-\frac{i}{\hbar} \frac{\Delta t}{2} H_1(t + \frac{\Delta t}{2})} \dots e^{-\frac{i}{\hbar} \frac{\Delta t}{2} H_{q-1}(t + \frac{\Delta t}{2})} \times e^{-\frac{i}{\hbar} \Delta t H_q(t + \frac{\Delta t}{2})} e^{-\frac{i}{\hbar} \frac{\Delta t}{2} H_{q-1}(t + \frac{\Delta t}{2})} \dots e^{-\frac{i}{\hbar} \frac{\Delta t}{2} H_1(t + \frac{\Delta t}{2})}, \quad (8)$$

such that evolution is then given by a product of small time steps

$$U(0, T) \approx \prod_{j=0}^{N-1} U_2(t_j + \Delta t) \quad (9)$$

with  $N$  the number of time steps,  $\Delta t = T/N$ , and  $t_j = j\Delta t$ . To extract the Berry phase from the circuit, we simply perform a Hadamard test on an auxiliary qubit (Fig. 1) [36, 37], where the Berry phase is extracted from the measurement statistics of the auxiliary qubit in the computational basis as

$$P(\sigma_z = +1) = \cos^2(\varphi_B/2). \quad (10)$$

In the following sections, the outlined methods are implemented for topological quantum magnets.

### III. TOPOLOGICAL INVARIANT OF FIRST ORDER 1D QUANTUM MAGNETS

The one-dimensional bond alternating spin-1/2 chain has been shown to host a rich phase diagram, including ferromagnetism, anti-ferromagnetism, Luttinger liquids, among others [48]. This system has been shown to reach a valence-bond ground state [49] with protected edge states [5]. Furthermore, dimerized systems can be realized in engineered systems, including spins on surfaces [50] and nano-graphene systems [51]. These systems can be described by the dimerized Heisenberg spin-1/2 model of the form

$$H = \sum_i J_i \mathbf{S}_i \cdot \mathbf{S}_{i+1} = \sum_i H_i, \quad (11)$$

where  $J_i = \{J_1 \text{ for even } i, J_2 \text{ for odd } i\}$  is the alternating bond strength, and  $\mathbf{S}_i$  is the vector of spin operators on lattice site  $i$ , whose entries are the Pauli matrices  $\mathbf{S} = \frac{\hbar}{2}(\sigma_x, \sigma_y, \sigma_z)$ . A bond can be gauged with a phase of the form [45, 52]

$$H_i \rightarrow \frac{1}{2} S_i^+ S_{i+1}^- e^{-i\varphi} + \frac{1}{2} S_i^- S_{i+1}^+ e^{i\varphi} + S_i^z S_{i+1}^z, \quad (12)$$

where  $S^\pm = \frac{\hbar}{2}(\sigma_x \pm \sigma_y)$  are the spin ladder operators. We make the phase time-dependent  $\varphi(t)$  and evolve the resulting time-dependent Hamiltonian in a loop according to Eq. 7 to obtain the Berry phase  $\varphi_B$ . Stronger bonds yield  $\varphi_B = \pi$  while weak bonds result in  $\varphi_B = 0$  (Fig. 2). The topological difference becomes evident when removing a strong bond, the resulting open boundary chain exhibits edge modes [53]. If a weak bond is removed, no edge modes appear. In the case of  $J_1 = J_2$  the system becomes degenerate during the evolution and no Berry phase can be defined [44].

The quantum circuit is built by first decomposing the Hamiltonian into time-dependent and time-independent parts  $H(t) = H_0 + H_1(t)$ . If the twist operation is on an

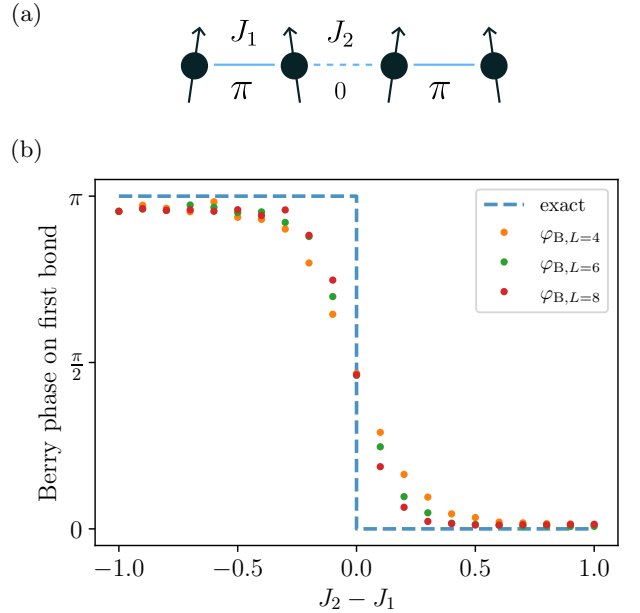


FIG. 2. (a) Schematic of a dimerized Heisenberg model featuring an SPT phase, with alternating bond strengths  $J_1$  and  $J_2$ , and their respective Berry phase for  $J_1 > J_2$ . (b) We show the Berry phase on the first bond as a function of the interaction strength difference  $J_2 - J_1$ , with a comparison to the exact solution (in blue). With increasing system size  $L$ , convergence towards the exact solution improves. A phase transition can be seen where the Berry phase  $\varphi_B$  changes from  $\pi \rightarrow 0$ , corresponding to topologically non-trivial and trivial states.

even (odd) bond, then the time independent part  $H_0$  will contain all odd (even) bonds. The time-dependent part contains only one non-commuting term at the twisted bond of the form  $H'_1(t) \propto \sigma^x \otimes \sigma^y - \sigma^y \otimes \sigma^x$ , so we split the time-dependent part  $H_1(t) = H'_1(t) + H''_1(t)$ , with  $H''_1(t)$  having the rest of the commuting terms. The decomposed Hamiltonian  $H(t) = H_0 + H'_1(t) + H''_1(t)$  is then used to approximate the time evolution as a second-order Trotter-Suzuki decomposition (cf. Eq. 8) [54]. A parameter sweep was performed for different dimer strengths  $J_2$ , setting  $J_1 = 1$ ,  $T = 20$ ,  $N = 200$ , and  $\hbar = 1$ . System sizes  $L = \{4, 6, 8\}$  were tested as well. The results are plotted in Fig. 2.

A phase transition can be seen at a bond when changing the relative strengths of the alternating pattern. The topological order parameter changes between 0 and  $\pi$ , corresponding to trivial and non-trivial phases. Errors increase when the link strengths approach each other and finite size effects become observable, yielding stronger deviations around  $J_2 - J_1 = 0$  from the exact value. Although the circuit shows promise, the circuit depths ranged around 100 000 layers. It is worth noting that due to the required depth, this circuit is not runnable on currently available quantum computers, requiring either substantially higher qubit fidelities, topological qubits or full error correction [55].

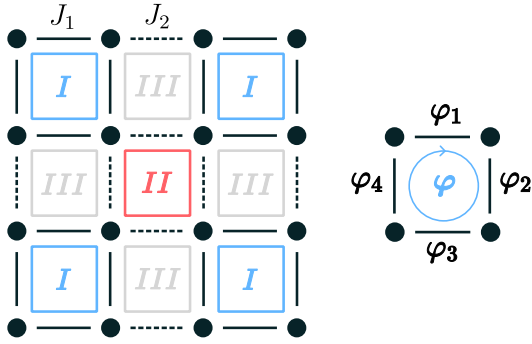


FIG. 3. Illustration of a two-dimensional tetramerized Heisenberg spin model and gauged twists, on an exemplary  $4 \times 4$  system. The alternating interaction strengths  $J_1$  and  $J_2$  are indicated by solid and dashed lines, respectively. This system exhibits a plaquette structure. Plaquettes of type I contain only nearest neighbor interactions of strength  $J_1$ , plaquettes of type II consist of strengths  $J_2$ , and plaquettes of type III are mixed. In order to calculate the Berry phase, we gauge a plaquette with four twists  $\varphi_j$  on each bond.

#### IV. TOPOLOGICAL INVARIANT OF SECOND ORDER 2D QUANTUM MAGNETS

We now study the two-dimensional SPT phase, a frustrated tetramerized square lattice spin-1/2 Heisenberg model. This model exhibits a rich phase diagram, including long-range order due to spontaneous symmetry breaking as well as higher-order topology [4, 50, 56]. This HOSPT phase has been experimentally realized with atomically engineered quantum spin lattices, including their topological corner modes [50]. The Hamiltonian takes the form

$$H = \sum_{\langle i,j \rangle} J_{ij} \mathbf{S}_i \cdot \mathbf{S}_j, \quad (13)$$

where the summation is over nearest neighbors and the interaction strengths  $J_{ij}$  have the valence-bond pattern with strengths  $J_1$  for plaquettes of type I and  $J_2$  for plaquettes of type II as shown in Fig. 3. Plaquettes of type III have mixed strengths, which are completely defined by the pattern of types I and II.

This model hosts a higher-order symmetry protected topological phase. The topological invariant for these types of phases are the  $\mathbb{Z}_Q$  invariants [57]. In the case of HOSPT phases with anti-unitary symmetry, the Berry phase invariant is still quantized to  $\{0, \pi\}$ . We can proceed analogously as in the previous section by adding a twist on each bond of the plaquette (cf. Eq. 12) [57]. The evolution becomes more complicated, since we must now traverse closed paths in a four-dimensional toroidal parameter space.

Defining plaquettes of type I as those which have stronger interaction strength  $J_1$  as compared to plaquettes of type II with weaker interaction  $J_2$ , twisting plaquettes of type I yields  $\varphi_B = \pi$  and of type II

yields  $\varphi_B = 0$ . The topological inequivalence follows analogously to the one-dimensional case. By "cutting" through plaquettes and considering the resulting open boundary system, splitting a type I plaquette will give corner modes while a type II will not [4, 57].

Similarly to the one-dimensional case, we can also find degeneracies when twisting the gauged plaquettes. An interesting result is that even for the decoupled case of  $J_2 = 0$ , some closed paths in parameter space yield an undefined Berry phase. During these paths, the energy gap between the ground state and the excited states closes, resulting in an undefined berry phase due to the degeneracy [44]. In this decoupled case, the four lowest energy levels of the spectrum of a single plaquette are of the form

$$E_{min} = -2J_1 \pm 2J_1 \left[ 5 \pm 4 \left| \cos \frac{|\varphi|}{2} \right| \right]^{1/2}, \quad (14)$$

where the twists are grouped into a vector  $\varphi = (\varphi_1, \varphi_2, \varphi_3, \varphi_4)$ , such that the parameter vector distance is  $|\varphi| = \sum_j \varphi_j$ . One can see that the ground state becomes degenerate whenever  $|\varphi| = \pi$ . Thus, valid parameter paths are loops in a 4-torus parameter space such that the distance is always  $|\varphi(t)| < \pi$ . A simple way to achieve this is to evolve parameters in opposite pairs  $\varphi_i(t) = -\varphi_j(t)$ , such that the vector distance is always canceled  $|\varphi(t)| = 0$ , ensuring that if the system starts in the ground state, it will always stay there during evolution.

The quantum circuit is built by dividing the Hamiltonian into the time-dependent part (which contains the twists) and time-independent part, such that  $H(t) = H_0 + H_1(t)$ . If the twist is on a plaquette of type I (type II), the time-independent part  $H_0$  will then consist of all  $J_2$  ( $J_1$ ) interactions, while the time-dependent  $H_1$  part contains all  $J_1$  ( $J_2$ ) interactions. These resulting parts are then split into vertical and horizontal interactions such that  $H_0 = H_{0,V} + H_{0,H}$ ,  $H_1(t) = H_{1,V}(t) + H_{1,H}(t)$ . Finally, both time-dependent parts are split by their non-commuting operators (given by the local twist evolution) as in the previous section such that  $H_{1,\alpha}(t) = H'_{1,\alpha}(t) + H''_{1,\alpha}(t)$ . This partition of the Hamiltonian is used to approximate the time evolution as a second-order Trotter-Suzuki decomposition (cf. Eq. 8) [58]. A parameter sweep was performed for different dimer strengths  $J_2$ , setting  $J_1 = 1$ ,  $T = 20$ , and  $N = \{100, 200, 300\}$ , and results are shown in Fig. 4. For this algorithm, the circuit depth was around 250 000 layers, which cannot be directly implemented in currently available quantum computers.

An interesting finding is that not all parameter paths yield the expected Berry phase. When only evolving two twists in a type I plaquette (leaving the other two stationary), we observed that twisting commuting links (i.e their spin bonds are not directly connected / interacting), the Berry phase would yield 0 rather than  $\pi$ . We summarize these findings in Table I. This result

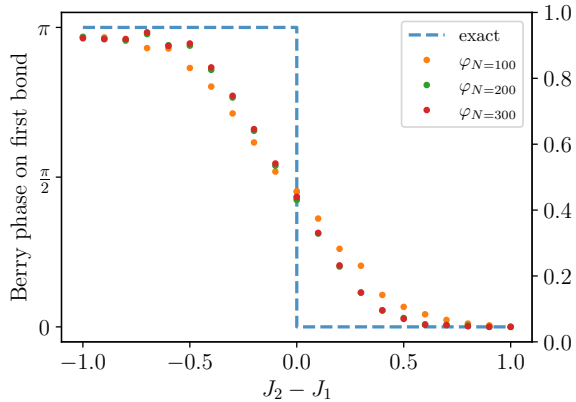


FIG. 4. Berry phase calculation on a plaquette as a function of the interaction strength difference  $J_2 - J_1$ , with a comparison to the exact solution (in blue). With increasing time steps  $N$ , convergence towards the exact solution improves. A phase transition can be seen where the Berry phase  $\varphi_B$  changes from  $\pi \rightarrow 0$ , corresponding to higher-order topologically non-trivial and trivial states.

Twisted pair Berry phase Commute		
$\varphi_1, \varphi_2$	$\pi$	No
$\varphi_1, \varphi_4$	$\pi$	No
$\varphi_2, \varphi_3$	$\pi$	No
$\varphi_3, \varphi_4$	$\pi$	No
$\varphi_2, \varphi_4$	0	Yes
$\varphi_1, \varphi_3$	0	Yes

TABLE I. Berry phase for a type I plaquette, only twisting two links. Twists on interactions that commute in the Hamiltonian do not yield the expected phase.

highlights an important feature, a higher-dimensional parameter geometry does not necessarily give the same topological charge when traversing it along different

closed paths. Gauging a symmetry and twisting the parameters can become non-trivial and one needs to carefully evolve through the introduced parameter space.

## V. CONCLUSION

In summary, we have presented a quantum algorithm that allows us to calculate topological invariants of a higher-order topological quantum magnet. Our algorithm relies on a high-dimensional path-dependent adiabatic evolution of the Berry phase, enabling the calculation of topological invariants in two-dimensional quantum many-body models. We uncover a hidden behavior of the invariant for different paths through the HOSPT parameter space, suggesting that gauging the symmetry has intricacies and one has to be careful how to define the invariant, a result which had been previously overlooked. Our results make a first step towards leveraging quantum computers to rationalize topology in many-body systems, including the nature of the quantum geometry formed by such parameter spaces of gauged HOSPT phases. It is finally worth noting that in the current formulation, the practical use of our algorithm requires substantial circuit depths and accurate ground state preparation, which are beyond the capabilities of currently available quantum computers. Our results highlight the potential for using future fault-tolerant or topological quantum computers to calculate topological invariants of HOSPT phases.

**Acknowledgments** We acknowledge the computational resources provided by the Aalto Science-IT project. We acknowledge the support from the Research Council of Finland through grants (Grant No. 370912), the European Research Council through ERC-CoG grant ULTRATWISTROICS (No. 101170477), InstituteQ, the Finnish Quantum Flagship, and the Jane and Aatos Erkko Foundation. We thank C. Flindt for useful discussions.

---

[1] J. E. Moore, The birth of topological insulators, *Nature* **464**, 194–198 (2010).

[2] X.-G. Wen, Colloquium: Zoo of quantum-topological phases of matter, *Rev. Mod. Phys.* **89**, 041004 (2017).

[3] C.-K. Chiu, J. C. Teo, A. P. Schnyder, and S. Ryu, Classification of topological quantum matter with symmetries, *Reviews of Modern Physics* **88**, 10.1103/revmodphys.88.035005 (2016).

[4] D. González-Cuadra, Higher-order topological quantum paramagnets, *Physical Review B* **105**, 10.1103/physrevb.105.1020403 (2022).

[5] H. Watanabe and L. Fu, Topological crystalline magnets: Symmetry-protected topological phases of fermions, *Physical Review B* **95**, 10.1103/physrevb.95.081107 (2017).

[6] X. Chen, Z.-X. Liu, and X.-G. Wen, Two-dimensional symmetry-protected topological orders and their protected gapless edge excitations, *Phys. Rev. B* **84**, 235141 (2011).

[7] X. Chen, Z.-C. Gu, and X.-G. Wen, Classification of gapped symmetric phases in one-dimensional spin systems, *Physical Review B* **83**, 10.1103/physrevb.83.035107 (2011).

[8] X.-G. Wen, Symmetry-protected topological phases in noninteracting fermion systems, *Physical Review B* **85**, 10.1103/physrevb.85.085103 (2012).

[9] Q.-R. Wang and Z.-C. Gu, Construction and classification of symmetry-protected topological phases in interacting fermion systems, *Physical Review X* **10**, 10.1103/physrevx.10.031055 (2020).

[10] W. A. Benalcazar, B. A. Bernevig, and T. L. Hughes, Quantized electric multipole insulators, *Science* **357**, 61–66 (2017).

[11] W. A. Benalcazar, B. A. Bernevig, and T. L. Hughes, Electric multipole moments, topological multipole moment pumping, and chiral hinge states in crystalline insulators, *Phys. Rev. B* **96**, 245115 (2017).

[12] Z. Song, Z. Fang, and C. Fang, D-2 -dimensional edge states of rotation symmetry protected topological states, *Physical Review Letters* **119**, 10.1103/physrevlett.119.246402 (2017).

[13] J. Langbehn, Y. Peng, L. Trifunovic, F. von Oppen, and P. W. Brouwer, Reflection-symmetric second-order topological insulators and superconductors, *Physical Review Letters* **119**, 10.1103/physrevlett.119.246401 (2017).

[14] F. Schindler, A. M. Cook, M. G. Vergniory, Z. Wang, S. S. P. Parkin, B. A. Bernevig, and T. Neupert, Higher-order topological insulators, *Science Advances* **4**, 10.1126/sciadv.aat0346 (2018).

[15] O. Dubinkin and T. L. Hughes, Higher-order bosonic topological phases in spin models, *Phys. Rev. B* **99**, 235132 (2019).

[16] A. Rasmussen and Y.-M. Lu, Classification and construction of higher-order symmetry-protected topological phases of interacting bosons, *Physical Review B* **101**, 10.1103/physrevb.101.085137 (2020).

[17] L.-Y. Hung and X.-G. Wen, Universal symmetry-protected topological invariants for symmetry-protected topological states, *Physical Review B* **89**, 10.1103/physrevb.89.075121 (2014).

[18] X.-G. Wen, Exactly soluble local bosonic cocycle models, statistical transmutation, and simplest time-reversal symmetric topological orders in 3+1 dimensions, *Physical Review B* **95**, 10.1103/physrevb.95.205142 (2017).

[19] Y. You, T. Devakul, F. J. Burnell, and T. Neupert, Higher-order symmetry-protected topological states for interacting bosons and fermions, *Phys. Rev. B* **98**, 235102 (2018).

[20] H. Song, S.-J. Huang, L. Fu, and M. Hermele, Topological Phases Protected by Point Group Symmetry, *Phys. Rev. X* **7**, 011020 (2017).

[21] S. Tamiya, S. Koh, and Y. O. Nakagawa, Calculating nonadiabatic couplings and berry's phase by variational quantum eigensolvers, *Physical Review Research* **3**, 10.1103/physrevresearch.3.023244 (2021).

[22] T. Kariyado, T. Morimoto, and Y. Hatsugai,  $Z_N$  Berry Phases in Symmetry Protected Topological Phases, *Phys. Rev. Lett.* **120**, 247202 (2018).

[23] O. Dubinkin and T. L. Hughes, Entanglement signatures of multipolar higher-order topological phases, *Physical Review B* **108**, 10.1103/physrevb.108.155138 (2023).

[24] C.-L. Deng, Y. Liu, Y.-R. Zhang, X.-G. Li, T. Liu, C.-T. Chen, T. Liu, C.-W. Lu, Y.-Y. Wang, T.-M. Li, C.-P. Fang, S.-Y. Zhou, J.-C. Song, Y.-S. Xu, Y. He, Z.-H. Liu, K.-X. Huang, Z.-C. Xiang, J.-C. Wang, D.-N. Zheng, G.-M. Xue, K. Xu, H. Yu, and H. Fan, High-order topological pumping on a superconducting quantum processor, *Physical Review Letters* **133**, 10.1103/physrevlett.133.140402 (2024).

[25] J. May-Mann, Y. You, T. L. Hughes, and Z. Bi, Interaction-enabled fractonic higher-order topological phases, *Physical Review B* **105**, 10.1103/physrevb.105.245122 (2022).

[26] Y. You, J. Bibo, and F. Pollmann, Higher-order entanglement and many-body invariants for higher-order topological phases, *Physical Review Research* **2**, 10.1103/physrevresearch.2.033192 (2020).

[27] J. F. Wienand, F. Horn, M. Aidelsburger, J. Bibo, and F. Grusdt, Thouless pumps and bulk-boundary correspondence in higher-order symmetry-protected topological phases, *Physical Review Letters* **128**, 10.1103/physrevlett.128.246602 (2022).

[28] Y. You, T. Devakul, F. J. Burnell, and T. Neupert, Higher-order symmetry-protected topological states for interacting bosons and fermions, *Physical Review B* **98**, 10.1103/physrevb.98.235102 (2018).

[29] C. Peng, L. Zhang, and Z.-Y. Lu, Deconfined quantum phase transition of a higher-order symmetry-protected topological state, *Phys. Rev. B* **104**, 075112 (2021).

[30] D. Azses, D. F. Mross, and E. Sela, Symmetry-resolved entanglement of two-dimensional symmetry-protected topological states, *Physical Review B* **107**, 10.1103/physrevb.107.115113 (2023).

[31] T. Ayral, P. Besserve, D. Lacroix, and E. A. Ruiz Guzman, Quantum computing with and for many-body physics, *The European Physical Journal A* **59**, 10.1140/epja/s10050-023-01141-1 (2023).

[32] Y. Liu, M.-Q. He, and Z. Wang, Variational quantum eigensolvers with quantum gaussian filters for solving ground-state problems in quantum many-body systems, *Physics Letters A* **555**, 130766 (2025).

[33] N. Yoshioka, M. Amico, W. Kirby, P. Jurcevic, A. Dutt, B. Fuller, S. Garion, H. Haas, I. Hamamura, A. Ivrii, R. Majumdar, Z. Minev, M. Motta, B. Pokharel, P. Rivero, K. Sharma, C. J. Wood, A. Javadi-Abhari, and A. Mezzacapo, Krylov diagonalization of large many-body hamiltonians on a quantum processor, *Nature Communications* **16**, 10.1038/s41467-025-59716-z (2025).

[34] C. Wille, O. Buerschaper, and J. Eisert, Fermionic topological quantum states as tensor networks, *Physical Review B* **95**, 10.1103/physrevb.95.245127 (2017).

[35] J. Ahn, S. Park, D. Kim, Y. Kim, and B.-J. Yang, Stiefel–whitney classes and topological phases in band theory, *Chinese Physics B* **28**, 117101 (2019).

[36] M. Niedermeier, M. Nairn, C. Flindt, and J. L. Lado, Quantum computing topological invariants of two-dimensional quantum matter, *Physical Review Research* **6**, 10.1103/physrevresearch.6.043288 (2024).

[37] B. Murta, G. Catarina, and J. Fernández-Rossier, Berry phase estimation in gate-based adiabatic quantum simulation, *Physical Review A* **101**, 10.1103/physreva.101.020302 (2020).

[38] K. Kudo, H. Watanabe, T. Kariyado, and Y. Hatsugai, Many-body chern number without integration, *Physical Review Letters* **122**, 10.1103/physrevlett.122.146601 (2019).

[39] A. Smith, B. Jobst, A. G. Green, and F. Pollmann, Crossing a topological phase transition with a quantum computer, *Physical Review Research* **4**, 10.1103/physrevresearch.4.1022020 (2022).

[40] X. Zhang, W. Jiang, J. Deng, K. Wang, J. Chen, P. Zhang, W. Ren, H. Dong, S. Xu, Y. Gao, F. Jin, X. Zhu, Q. Guo, H. Li, C. Song, A. V. Gorshkov, T. Iadecola, F. Liu, Z.-X. Gong, Z. Wang, D.-L. Deng, and H. Wang, Digital quantum simulation of floquet symmetry-protected topological phases, *Nature* **607**, 468–473 (2022).

[41] J. M. Koh, T. Tai, and C. H. Lee, Realization of higher-

order topological lattices on a quantum computer, *Nature Communications* **15**, 10.1038/s41467-024-49648-5 (2024).

[42] R.-Y. Sun, T. Shirakawa, and S. Yunoki, Efficient variational quantum circuit structure for correlated topological phases, *Physical Review B* **108**, 10.1103/physrevb.108.075127 (2023).

[43] J. C. Solem and L. C. Biedenharn, Understanding geometrical phases in quantum mechanics: An elementary example, *Foundations of Physics* **23**, 185–195 (1993).

[44] D. Xiao, M.-C. Chang, and Q. Niu, Berry phase effects on electronic properties, *Reviews of Modern Physics* **82**, 1959–2007 (2010).

[45] Y. Hatsugai, Quantized berry phases as a local order parameter of a quantum liquid, *Journal of the Physical Society of Japan* **75**, 123601 (2006).

[46] N. Hatano and M. Suzuki, Finding exponential product formulas of higher orders, in *Quantum Annealing and Other Optimization Methods* (Springer Berlin Heidelberg, 2005) p. 37–68.

[47] M. SUZUKI, General decomposition theory of ordered exponentials., *Proceedings of the Japan Academy, Series B* **69**, 161–166 (1993).

[48] Q. Luo, J. Zhao, X. Wang, and H.-Y. Kee, Unveiling the phase diagram of a bond-alternating spin- $\frac{1}{2}$   $K$ - $\Gamma$  chain, *Physical Review B* **103**, 10.1103/physrevb.103.144423 (2021).

[49] S. Sachdev, Quantum magnetism and criticality, *Nature Physics* **4**, 173–185 (2008).

[50] H. Wang, P. Fan, J. Chen, L. Jiang, H.-J. Gao, J. L. Lado, and K. Yang, Construction of topological quantum magnets from atomic spins on surfaces, *Nature Nanotechnology* **19**, 1782–1788 (2024).

[51] C. Zhao, G. Catarina, J.-J. Zhang, J. C. G. Henriques, L. Yang, J. Ma, X. Feng, O. Gröning, P. Ruffieux, J. Fernández-Rossier, and R. Fasel, Tunable topological phases in nanographene-based spin-1/2 alternating-exchange heisenberg chains, *Nature Nanotechnology* **19**, 1789–1795 (2024).

[52] Y. Hatsugai, Quantized berry phases for a local characterization of spin liquids in frustrated spin systems, *Journal of Physics: Condensed Matter* **19**, 145209 (2007).

[53] J. L. Lado, R. Ortiz, and J. Fernández-Rossier, Emergent quantum matter in graphene nanoribbons, in *Graphene Nanoribbons*, 2053–2563 (IOP Publishing, 2019) pp. 4–1 to 4–21.

[54] The circuit was implemented using Qiskit’s AerSimulator [59] with 100 000 shots. As outlined in Ground state preparation was done using Qiskit’s state preparation method.

[55] J. Preskill, Quantum computing in the nisq era and beyond, *Quantum* **2**, 79 (2018).

[56] P. M. Vecsei and J. L. Lado, Phase diagram of the  $j_1$ – $j_2$  heisenberg second-order topological quantum magnet, *Phys. Rev. Res.* **7**, 013194 (2025).

[57] H. Araki, T. Mizoguchi, and Y. Hatsugai,  $\mathbb{Z}_Q$  berry phase for higher-order symmetry-protected topological phases, *Physical Review Research* **2**, 10.1103/physrevresearch.2.012009 (2020).

[58] We implemented this circuit for a  $4 \times 4$  spin system, using Qiskit’s AerSimulator [59] with 100 000 shots.

[59] A. Javadi-Abhari, M. Treinish, K. Krsulich, C. J. Wood, J. Lishman, J. Gacon, S. Martiel, P. D. Nation, L. S. Bishop, A. W. Cross, B. R. Johnson, and J. M. Gambetta, *Quantum computing with qiskit* (2024).